Ab initio electronic and magnetic structure in $La_{0.66}Sr_{0.33}MnO_3$: strain and correlation effects

2006 J. Phys.: Condens. Matter 18 7717

(http://iopscience.iop.org/0953-8984/18/32/019)

INSTITUTE OF PHYSICS PUBLISHING JOURNAL OF PHYSICS: CONDENSED MATTER

J. Phys.: Condens. Matter **18** (2006) 7717–7728 doi:10.1088/0953-8984/18/32/019

Ab initio electronic and magnetic structure in $La_{0.66}Sr_{0.33}MnO_3$: strain and correlation effects

Chunlan Ma[1,2], Zhongqin Yang[1] and Silvia Picozzi[3]

[1] Surface Physics Laboratory (National Key Laboratory), Fudan University, Shanghai 200433, People's Republic of China
[2] Department of Applied Physics, University of Science and Technology of Suzhou, Suzhou 215011, People's Republic of China
[3] CNR-INFM, CASTI Regional Laboratory, 67100 Coppito (L'Aquila), Italy

E-mail: silvia.picozzi@aquila.infn.it

Received 24 May 2006, in final form 13 July 2006
Published 31 July 2006
Online at stacks.iop.org/JPhysCM/18/7717

Abstract

The effects of tetragonal strain on the electronic and magnetic properties of strontium-doped lanthanum manganite, $La_{2/3}Sr_{1/3}MnO_3$ (LSMO), are investigated by means of density-functional methods. As far as the structural properties are concerned, the comparison between theory and experiments for LSMO strained on the most commonly used substrates shows an overall good agreement: the slight overestimate (at most of 1–1.5%) for the equilibrium out-of-plane lattice constants points to possible defects in real samples. The inclusion of a Hubbard-like contribution on the Mn d states, according to the so-called 'LSDA + U' approach, is rather ineffective from the structural point of view, but much more important from the electronic and magnetic point of view. In particular, full half-metallicity, which is missed within a bare density-functional approach, is recovered within LSDA + U, in agreement with experiments. Moreover, the half-metallic behaviour, particularly relevant for spin-injection purposes, is independent of the chosen substrate and is achieved for all the considered in-plane lattice constants. More generally, strain effects are not seen to crucially affect the electronic structure: within the considered tetragonalization range, the minority gap is only slightly (i.e. by about 0.1–0.2 eV) affected by a tensile or compressive strain. Nevertheless, we show that the growth on a smaller in-plane lattice constant can stabilize the out-of-plane versus in-plane e_g orbital and significantly change their relative occupancy. Since e_g orbitals are key quantities for the double-exchange mechanism, strain effects are confirmed to be crucial for the resulting magnetic coupling.

(Some figures in this article are in colour only in the electronic version)

1. Introduction

Strontium-doped lanthanum manganites, $La_{1-x}Sr_xMnO_3$, have been much studied in the past few decades [1–3], due to their fascinating properties and intriguing applications. Nevertheless, most of the properties are composition dependent, and the most exotic ones, such as colossal magnetoresistance and/or half-metallicity, appear only when $0.17 < x < 0.5$ [2]. In the case of the optimized composition ($x \sim 1/3$), $La_{0.66}Sr_{0.33}MnO_3$ (denoted as LSMO hereafter) shows a spin polarization >95% [4] and a high Curie ferromagnetic temperature ($T_C \sim 370$ K); therefore, this compound appear as a promising candidate in the spin injection framework, especially since it is envisaged that LSMO-based devices could operate at room temperature.

The interactions between electrons and lattice distortions are well known to play a significant role in the physics of the compound: Mn e_g electrons, which are responsible for the rich variety of attractive properties shown by manganites, are coupled to the lattice through Jahn–Teller effects [5]. In particular, MnO_6 octahedral tetragonal distortions can be induced by the lattice mismatch between the film and the substrate, to which magnetic anisotropy and magnetoresistance effects of LSMO films were found to be extremely sensitive [6]. In particular, the magnetization easy axis was shown to move from in-plane to out-of-plane upon moving from tensile to compressive strain [7, 8]. Moreover, it is mandatory for industrial applications to achieve a good control over the film growth, which in turn requires a careful choice of appropriate substrates to get optimized LSMO films. High-performance epitaxial manganite thin films have been successfully grown on [001]-oriented oxides, such as $LaAlO_3$ (LAO) [6, 9], $La_{0.3}Sr_{0.7}Al_{0.35}Ta_{0.35}O_9$ (LSAT) [6], $NdGaO_3$ (NGO) [6], and $SrTiO_3$ (STO) [4, 10, 11]. Strained manganite epilayers often show a different behaviour with respect to the bulk. In particular, for LSMO, tensile strain was shown to reduce the Curie ordering temperature, T_C, and this was successfully explained in terms of double exchange: the increase of the in-plane Mn–O bond length leads to a reduction of the hopping term between Mn^{3+}–Mn^{4+}, therefore reducing T_C (see below) [5]. However, for other manganites, such as $La_{1-x}Ba_xMnO_3$, a tensile strain was found to enhance T_C [12]. Therefore, a thorough understanding has not yet been achieved, due to contradictory results. Possible reasons might include the still poor control over the sample growth and stoichiometry. Moreover, one should keep in mind that the delicate interplay between charge, spin and orbital ordering can be very easily altered in manganites and the subtleties of the relevant physical effects (such as magnetoresistance and anisotropy) can lead to strikingly different results induced by generally tiny changes.

Despite the large abundance of experimental studies devoted to substrate-induced strain effects on the LSMO magnetic properties [6, 9] and *ab initio* theoretical works focused on LSMO [13–17], a deep investigation of strain effects on the electronic and magnetic properties from first principles (both with and without additional correlation effect beyond standard exchange–correlation functionals) is lacking and will therefore be the focus of the present work. We choose four typical substrates whose mismatches with LSMO films induce different types of lattice strain: LAO, for which the film undergoes a relatively large in-plane compressive strains; LSAT and NGO, for which the film undergoes a very small compressive strain; and STO, for which the film experiences a small tensile strain. The paper is organized as follows. In section 2 we report some technicalities (in terms of structural and computational details); in section 3 we focus on the structural equilibrium properties of LSMO strained on different substrates. Then, we move in section 4 to the discussion of the effects of strain and correlation on the LSMO electronic and magnetic properties, in terms of density of states and magnetic moments. Finally, we summarize our conclusions in section 5.

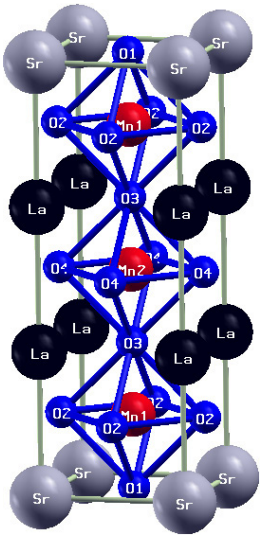

Figure 1. Schematic unit cell (Bravais lattice shown by thin solid lines) for LSMO: grey, blue, red and black spheres denote Sr, O, Mn and La atoms, respectively. The vertical axis shows the [001] direction. O–O bonds are shown via blue rods.

2. Crystal structure and computational details

Our calculations are performed following the generalized gradient approximation (GGA) [18] to the exchange–correlation potential within the framework of density functional theory (DFT), using the all-electron full-potential linearized augmented plane-wave (FLAPW) [19] method as implemented in the FLEUR code [20]. In order to take into account correlation effects beyond the local spin density approximation (LSDA) or the GGA, we used the so-called 'LSDA + U' (or 'GGA + U', in this case) scheme [21] in the 'atomic limit' approximation, as implemented in FLEUR [22]; this formalism includes a Hubbard-like potential acting on the Mn 3d states that enhances the tendency towards localization which erroneously is lacking in bare GGA.

The unit cell is divided into non-overlapping spheres and an interstitial region. The muffin-tin (MT) radii are set to 2.5 au for Sr and La, 2.0 au for Mn and 1.5 au for O, respectively. The wavefunction expansion in the interstitial region was carried up to $\mathbf{k}_{\max} = 3.8$ au^{-1}, which limits the number of basis functions to be 600 or so. We treated the La 5s, 5p and Sr 4s, 4p states as local-orbital states [23], whereas the La 4f states were treated as valence states. The energy position of these latter states (resulting to be at $\sim$2 eV above the Fermi level, see below) can be questionable and might be an artefact of DFT-FLAPW; however, tests made applying a large Coulomb parameter ($U = 10$ eV) on La 4f states show that the effect on the physical quantities we are mainly interested in (i.e. total energies and density of occupied states) is negligible.

In order to sample the irreducible Brillouin zone, 72 **k**-points were used, according to the $12 \times 12 \times 4$ Monkhorst–Pack shell [24]; the convergency with respect to this parameter was accurately tested. Within the GGA + U formalism, we considered different values of U (such as 2 and 3 eV), which were found to give the better agreement of DFT results with recent photoemission measurements [25]. The J value was set to $J = 0.7$ eV.

In order to simulate LSMO, we used a 15-atom unit cell which can be schematically represented as a [001]-ordered $(SrMnO_3)_1/(LaMnO_3)_2$ superlattice (see figure 1), similar to

Table 1. Experimental and theoretical structural parameters for LSMO films grown on different substrates: in-plane lattice constants (a, in Å), out-of-plane lattice constants (c, in Å), c/a ratio and unit-cell volume (V, in Å^3). Experimental values are taken from [6]. In parentheses, we report the in-plane and out-of-plane strain components defined as $\epsilon_{xx} = (a-a_{\rm eq})/a_{\rm eq}$ and $\epsilon_{zz} = (c-a_{\rm eq})/a_{\rm eq}$, respectively. Strains are evaluated with respect to the ideally unstrained experimental cubic lattice constant ($a_{\rm eq} = c_{\rm eq} = 3.874$ Å).

		c (ϵ_{zz})		c/a		V	
Substrate	a (ϵ_{xx})	Expt	Th.	Expt	Th.	Expt	Th.
LAO	3.793 (−2.1%)	3.991 (3.0%)	3.971	1.052	1.048	57.42	57.19
NGO	3.861 (−0.3%)	3.902 (0.7%)	3.927	1.011	1.017	58.17	58.54
LSAT	3.868 (−0.1%)	3.892 (0.5%)	3.924	1.006	1.014	58.23	58.71
STO	3.905 (0.8%)	3.850 (−0.6%)	3.899	0.986	0.999	58.71	59.47

previous works [13]. With this choice of unit cell, there are two inequivalent Mn: Mn_1 has a LaO plane on one side and a SrO plane on the other side, whereas Mn_2 has LaO layers on both sides. Possible MnO_6 octahedral tiltings were neglected. Effects induced by this approximation are quantitatively hard to predict; moreover, experiments suggest the tilting angle not to be strongly affected by different strain conditions [26]. The in-plane lattice constants a are chosen according to the LAO, NGO, LSAT and STO bulk experimental values [6]; this is of course an approximation, and the theoretical substrate lattice constants might be used, as well. In some cases (i.e. when the disagreement between the theoretical and experimental lattice constants for the substrate or for the epilayer is rather high), one or the other choice can lead to different strain signs and qualitatively different behaviour. However, in the present case, when considering LSMO grown on different substrates, the choice of the experimental substrate lattice constants does not change the strain sign with respect to the experimentally realized situation. In fact, the LSMO equilibrium calculated (see below) and experimental 'cubic' lattice constant are $a_{\rm eq}^{\rm th} = 3.90$ Å and $a_{\rm eq}^{\rm expt} = 3.874$ Å, respectively. Therefore, in both simulations and experiments, the epilayer is under tensile strain for STO and under compressive strain in the other cases. The out-of-plane lattice parameters c have been set to (i) experimental values for LSMO thin films [6] grown on different substrates and (ii) minimized according to the calculated total energies (see below). To test the effect of structural optimization, we relaxed the atomic positions of LSMO strained on STO until the forces were less than 0.002 Hartree au^{-1}. We verified that the electronic structure is negligibly affected by structural optimization of internal atomic coordinates; therefore, we will focus in the following on the unrelaxed structures. In all the simulations, the three Mn atoms in the unit cell were aligned ferromagnetically, according [2] to experiments[4].

3. Structural equilibrium properties

In figure 2 we show the total energy versus out-of-plane lattice constant for different substrates (see panels (b), (c), (d) and (e) for $LSMO_{LAO}$, $LSMO_{NGO}$, $LSMO_{LSAT}$ and $LSMO_{STO}$, respectively); we performed a parabolic fit of the total energies and obtained the equilibrium c as the parabola minimum for each different substrate. The resulting c values are then plotted in figure 2(a) as a function of the substrate lattice constants and compared with corresponding experimental values. Similarly, in table 1 we report the in-plane lattice constants (a) for the different chosen substrates, as reported in [6], along with the corresponding

[4] The stability of the ferromagnetic versus competitive phases (such as often occurring so-called 'CE' [2]) as a function of strain—though representing a very interesting topic—goes beyond the scope of this manuscript.

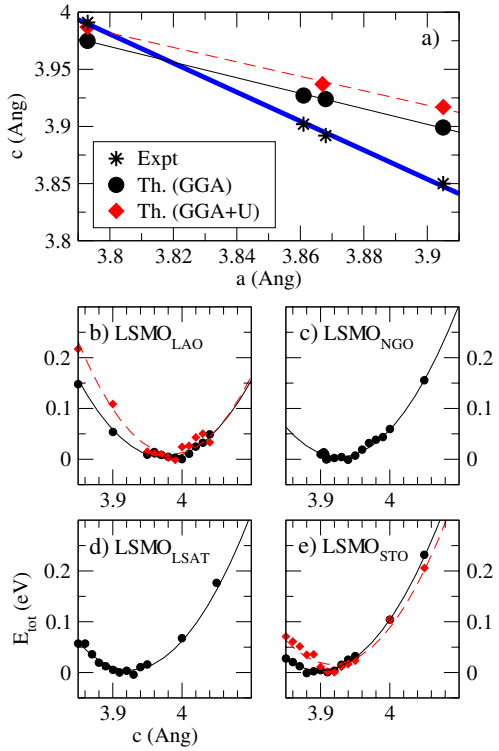

Figure 2. (a) Out-of-plane lattice constants (denoted as c) versus in-plane lattice constant (denoted as a): experimental values, GGA and GGA + U results are shown as black stars, black filled circles and red filled diamonds, respectively. Linear fits to each set of data are also shown. The total energy curves as a function of c are shown (with black symbols and solid lines) for different substrates in panels (b), (c), (d) and (e) for $LSMO_{LAO}$, $LSMO_{NGO}$, $LSMO_{LSAT}$ and $LSMO_{STO}$, respectively. In (b) and (e), the red symbols and dashed line show the results of GGA + U calculations ($U = 2$ eV). Axis labels in panels (b), (c) and (e) (not reported for clarity in plotting) are the same as (d).

experimental and theoretical values for the out-of-plane lattice constant (c), the strain components (ϵ_{ii}), and the c/a ratio as well as the resulting volume (V). The experimental LSMO equilibrium (i.e. unstrained) lattice constant was estimated as the weighted average between the experimental lattice parameter of the constituents, $LaMnO_3$ and $SrMnO_3$, and is evaluated as $a_{eq} = 3.874$ Å [10].

First of all, as expected from elasticity theory, the c parameter decreases as the strain becomes more and more tensile. However, both from the theoretical and experimental point of view, the lack of a constant volume shows that the material does not behave as an ideal elastic medium: the more compressive (tensile) is the strain, the smaller (larger) is the volume. Moreover, we see from figure 2(a) that, in the range of substrate lattice constants considered, the c versus a relation is well described using a linear fit, both for theoretical as well as experimental values. However, the slope of the experimental results is larger than the theoretical one. In particular, GGA slightly overestimates the c parameter in all cases (at most by 1.3%), except for $LSMO_{LAO}$. This can be interpreted as follows: on the one hand, the slight disagreement between experimental and theoretical c values might be due to non-perfect experimental samples. In fact, it is well known that twin-like defects [10] or oxygen lack—or excess—can often occur as a result of the different growth conditions. The experimental

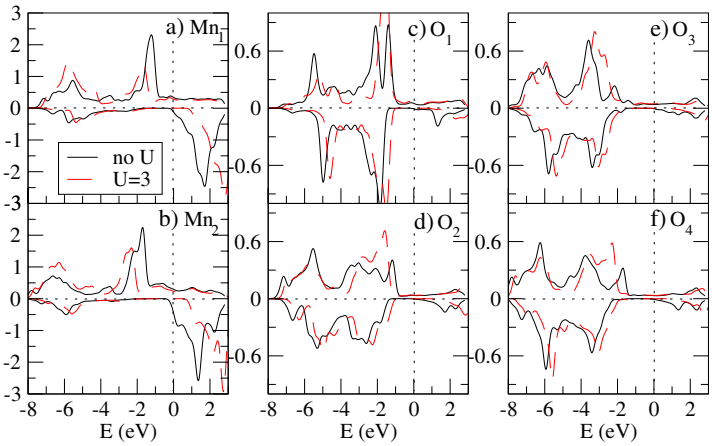

Figure 3. PDOS for (a) Mn_1, (b) Mn_2, (c) O_1, (d) O_2, (e) O_3 and (f) O_4 for $LSMO_{LAO}$. Black solid and red dashed lines show the results of GGA and GGA $+ U$ calculations, respectively ($U = 3$ eV). Atomic labels are consistent with figure 1.

films might therefore show a non-perfect stoichiometry or a non-high-quality crystallinity (at variance with our simulated perfect crystal), therefore resulting in slightly different lattice constants. On the other hand, we have to keep in mind that GGA is known to describe rather well (i.e. within 1–2%) the structural properties of magnetic systems (generally better than LSDA), though showing in some cases a slight overestimation of the lattice constants. This could be the case, although the disagreement with experiments is within the generally acknowledged error range. Therefore, in order to check whether the error is due to the neglect of correlation effects, we repeated the calculations for the LAO and STO substrates (see red diamonds and dashed lines in figures 2(b) and (e), respectively), using a GGA + U approach with $U = 2$ eV. In both cases, we found a slight increase of the c parameter, which brings LAO in excellent agreement with experiments, but STO to an even worse value. Our results are perfectly consistent with previous studies on other magnetic oxides [27]: the addition of a Hubbard-like potential to bare LSDA or GGA generally leads to only slight changes in the structural properties (and in particular to a larger volume, consistently with our results), though it is generally much more 'effective' from the electronic structure point of view, bringing about a much closer agreement with spectroscopic properties, compared to GGA (see below).

4. Electronic and magnetic structure

Before starting the discussion of strain-induced effects on the magnetic and electronic properties, we briefly comment on one of the systems of interests, namely LSMO strained on LAO, in terms of density of states and magnetic moments. Next, we will focus on the comparison between this same system and others under different strain conditions (i.e. different substrate lattice constants), according to the experimental equilibrium structure; finally, we will focus on the systems on a fixed in-plane lattice constant and study the effects of the c elongation.

4.1. Electronic and magnetic structure of LSMO strained on LAO: hybridization and correlation effects

We show in figure 3 the $LSMO_{LAO}$ density of states projected (PDOS) on the relevant atoms: Mn and O. As is well known, La and Sr only donate their electrons to the electronic system, the

bonding being dictated essentially by the Mn–O interaction [13]. In fact, as is clearly visible in figure 3, there is a strong hybridization between Mn d and O p states, especially in the majority occupied states. The peak at binding energies at -1.2 and $+1.8$ eV show the t_{2g} orbitals (not so strongly mixed), whereas the remaining part of the Mn PDOS shows the e_g contributions, much broader due to hybridization. As can be also seen from the PDOS, and will be better clarified in the following, the system is 'nearly half-metallic', i.e. it shows a gap of ∼1–2 eV (see below), but the conduction band minimum (CBM) is just below the Fermi level (E_F). Therefore, the system is not strictly 100% spin-polarized at E_F.[5] The situation changes upon introduction of the Coulomb correlations on the Mn 3d states: as is shown in figure 3 in the case of $U = 3$ eV, the system becomes fully half-metallic, consistently with experiments, suggesting a degree of spin-polarization larger than 95% [4]. As expected, the occupied (unoccupied) d states are shifted towards higher binding (higher excited) energies by about 1 eV (i.e. of the order of $(U - J)/2$) and, due to the strong hybridization, O p states are also affected (see figures 3(c)–(f)). Therefore, since within bare GGA half-metallicity is broken because the tails of minority Mn d states cross E_F, the Hubbard-induced shift towards higher energies results in a fully half-metallic character for $LSMO_{LAO}$.

As for the magnetic moments, we recall [28, 13] that the two Mn atoms are surrounded by different cationic environments: Mn_1 has a LaO plane on one side and a SrO plane on the other side, whereas Mn_2 has LaO layers on both sides. As a result, the magnetic moment of Mn_2 (3.26 μ_B) is closer to pure $LaMnO_3$ in similar strain conditions (i.e. of the order of 3.3 μ_B), whereas the moment of Mn_1 (3.11 μ_B) is, as expected, lower than Mn_2, but somewhat larger than the average of $LaMnO_3$ and $SrMnO_3$ (this latter showing a muffin-tin moment of about 2.7 μ_B). The changes in the electronic structure induced by the presence of additional correlations (and in particular the shift of Mn d states towards higher binding energies) affect in turn the magnetic moments: whereas, in the bare GGA case, the total magnetic moment is 10.89 μ_B, this increases up to 11.0 μ_B, when the GGA + U approach is used. The integer total magnetic moment is consistent with the fully half-metallic character previously outlined. Similarly, the atomic moments increase up to 3.29 and 3.49 μ_B for Mn_1 and Mn_2, respectively. However, neither within GGA nor within GGA + U is the picture of charge ordering and mixed Mn^{3+} and Mn^{4+} valences valid within the present DFT-based formalism and with the present considered unit cell, as already outlined in previous papers [13]. Finally, we remark that the magnetic moment is about 3.66 μ_B/Mn, in rather good agreement with experimentally reported values of 3.7 μ_B [10].

4.2. Strain effects on the electronic and magnetic structure

Let us now focus on the structures grown on different substrates at the experimental a and c lattice constants (see table 1). In figure 4 we report the total density of states (TDOS) of LSMO under tensile and compressive strains. The TDOS for LSMO grown on NGO looks very similar to LSMO grown on LSAT and is therefore not shown.

The comparison shows that the TDOSs all look rather similar. However, one can note that, in going from compressive to tensile strain, the band structure (both in the majority and minority spin channels) shifts towards lower binding energies (by ∼few tenths of eV for the considered strains of few per cents). Furthermore, in none of the considered substrates does the system show full half-metallicity; rather, all of them are 'nearly' half-metallic. In order to further investigate the role of strain on the half-metallic behaviour, we report in figure 5 the energy position (taking E_F as reference) of the valence band maximum (VBM) and of the CBM

[5] We observe that, if the La 4f states are treated within LSDA + U ($U = 10$ eV), changes in the Mn d unoccupied states around 2–3 eV are expected, but the half-metallic versus 'nearly' half-metallic character is unaffected.

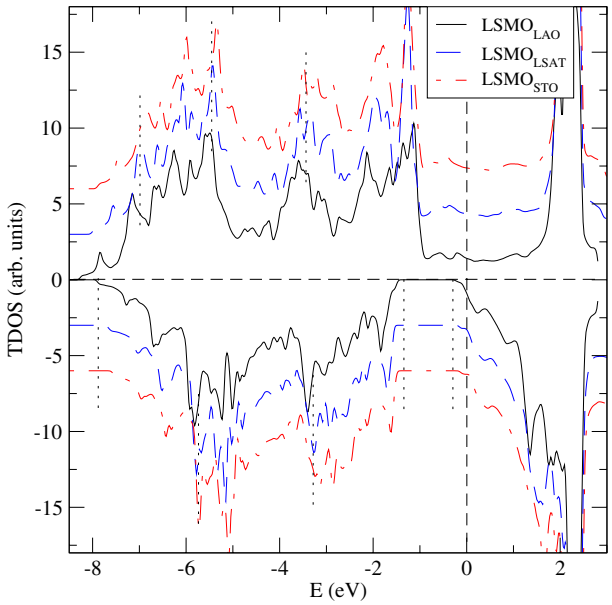

Figure 4. TDOS for LSMO grown on LAO (black solid line), LSAT (blue dashed line) and STO (red dot–dashed line)with GGA method. The zero of the energy scale is set to the Fermi level. Majority (minority) spin contributions are shown in the positive (negative) y-axis. For clarity, the TDOSs in the case of $LSMO_{STO}$ and $LSMO_{LSAT}$ are arbitrarily shifted along the y-axis. Vertical dotted lines are guides to the eyes.

in the minority spin channel as a function of the substrate lattice constant. The plots show that, in all the considered systems, the CBM is always lower than E_F, therefore hindering the full half-metallicity. However, there is a slight tendency towards half-metallicity upon applying a tensile strain: LSMO grown on STO is closer to half-metallicity than LSMO grown on LAO. Furthermore, the minority band gap slightly increases with the substrate lattice constant.

Let us now focus on the effects of correlation and of strain on the bandgap and of the relative position of E_F with respect to the minority band edges. Upon introduction of U and already for a small value $U = 2$ eV, the Fermi level enters the gap. As expected, the gap (here defined as the difference between the CBM and the VBM, irrespective of the position of E_F) increases with applying progressively increasing U parameters: within the range of considered strains (i.e. in going from $LSMO_{LAO}$ to $LSMO_{STO}$), it is of the order of 1.2–1.4 eV within bare GGA, of 1.6–1.8 eV within GGA + U ($U = 2$ eV) and of 1.9–2.1 eV within GGA + U ($U = 3$ eV). On the other hand, no significative changes are observed upon applying strains (at least in the experimentally accessible range): the strain-induced effects on the gap-magnitude amount at most to 0.1–0.2 eV.

It is of further interest to investigate the effects on the strain of the magnetic properties, in terms of magnetic moments. In going from $LSMO_{LAO}$ to $LSMO_{STO}$, the Mn_1 and Mn_2 moments range from 3.11 to 3.15 μ_B and from 3.26 to 3.29 μ_B, respectively. In parallel, the total moment ranges from 10.89 to 10.94 μ_B. Therefore, consistently with the slight changes in the electronic structure, the magnetic moments only slightly increase upon increasing the substrate lattice constant.

Since the physics of LSMO crucially depends on the e_g orbitals, whose occupancy and itineracy strongly affect the resulting ferromagnetism through double exchange, we further investigate the Mn d PDOS, further resolved by m character. We recall that in a cubic symmetry,

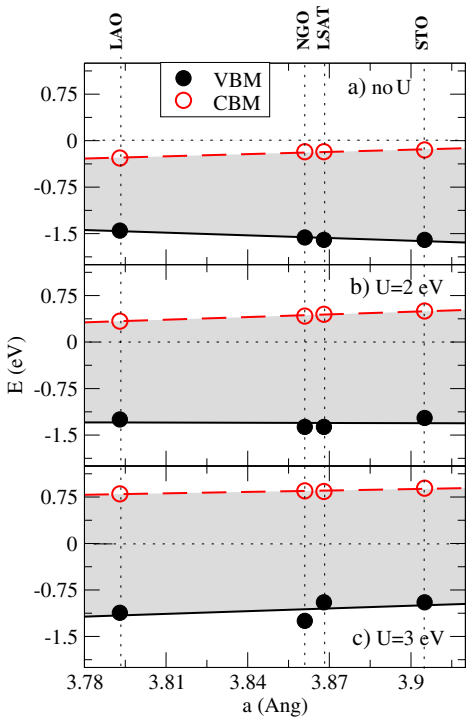

Figure 5. CBM (red empty circles) and VBM (black filled circles) positions in the minority spin channel with respect to E_F (set to zero) as a function of the in-plane lattice constant (labels on top show the experimentally considered substrates). Panels (a), (b) and (c) show the results of bare GGA, GGA + U ($U = 2$ eV) and GGA + U ($U = 3$ eV) approaches, respectively.

the e_g level is twofold degenerate; however, upon tetragonal strain, the degeneracy is lifted and the $x^2 - y^2$ in-plane orbital becomes different from the $3z^2 - r^2$ out-of-plane orbital. Therefore two competing mechanisms are induced by strain: (i) on the one hand, according to double exchange, T_C is proportional to the transfer integral t_0, describing the Mn^{3+}–Mn^{4+} hopping through intervening oxygen atoms. In turn, $t_0 \propto d_0^{-3.5}$, where d_0 is the in-plane Mn–O bond length. Therefore, a tensile strain, which increases the in-plane d_0, should reduce t_0, and, as a consequence, T_C; (ii) on the other hand, the relative occupancy of the $x^2 - y^2$ and $3z^2 - r^2$ orbitals also depends on strain: in particular, for a tensile strain, the occupancy of the in-plane orbital should be higher than that of the out-of-plane orbital. In parallel, the $x^2 - y^2$ has a larger transfer intensity: the stabilization and related increased occupation of this orbital therefore enhances electron hopping and, therefore, T_C. The investigation of the strain dependence of ferromagnetic coupling and of T_C goes beyond the scope of the present work. However, we provide here some hints on the occupation of the $x^2 - y^2$ and $3z^2 - r^2$ orbitals, which could serve as a starting point for further investigations on the magnetism in LSMO under strain conditions.

In figure 6, we show the orbital-resolved DOS projected on the two e_g orbitals for $LSMO_{STO}$ and $LSMO_{LAO}$ (both with and without the inclusion of the Hubbard parameter U) for the two inequivalent Mn_1 and Mn_2 atoms. We also show the integral of the PDOS, defined, for example for the in-plane e_g orbital of Mn_1, as $I^{Mn_1}_{x^2-y^2}(E) = \int^E \mathrm{PDOS}_{x^2-y^2}(E')\,\mathrm{d}E'$. This is particularly meaningful for $E = E_F$, where the integral coincides with the occupation of the

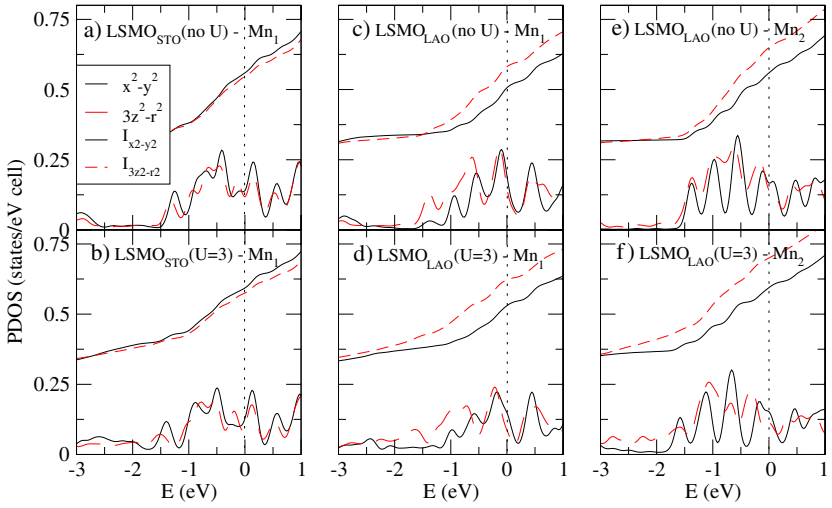

Figure 6. Mn_1 PDOS of $x^2 - y^2$ (black bold solid) and $3z^2 - r^2$ (red bold dashed) for LSMO on (a) STO within GGA, (b) STO within GGA + U ($U = 3$ eV), (c) LAO within GGA and (d) LAO within GGA + U. The Mn_2 PDOS of $x^2 - y^2$ (black bold solid) and $3z^2 - r^2$ (red bold dashed) for LSMO on (e) LAO within GGA and (f) LAO within GGA + U ($U = 3$ eV). Also shown are the integrals: $I^{Mn}_{x^2-y^2}(E)$ (black thin solid) and $I^{Mn}_{3z^2-r^2}(E)$ (red thin dashed).

orbital. Note that the t_{2g} orbitals as well are affected by strain and the three-fold degeneracy is lifted. However, their occupation is not modified upon tetragonal distortion: in fact, their PDOS (not reported) shows a peak in the $[-1.5{:}-1]$ eV range and becomes negligible above ~ -0.5 eV, resulting in full occupation of the majority subband contributions. On the other hand, minority t_{2g} states are completely unoccupied (as already mentioned, their tails slightly cross E_F but this is likely to be an artefact of DFT and full zero-occupation, i.e. half-metallicity, can be restored by applying an additional Coulomb correlation). It is evident from figure 6(a) that, even in $LSMO_{STO}$, showing an in-plane tensile strain of $+0.8\%$, the degeneracy is lifted, but the consequences are still small: as expected, the in-plane e_g is more occupied, but only by about 0.01 electrons more than in the out-of-plane e_g case. This picture is kept more or less unaltered even upon application of U (see figure 6(b)). On the other hand, if we look at $LSMO_{LAO}$, where the strain is markedly compressive, there is a considerable difference between the occupations of the e_g orbitals and the situation is reversed with respect to tensile strain: the $3z^2 - r^2$ is about 15% more occupied than $x^2 - y^2$ for Mn_1 within bare GGA (cf figure 6(c)) and this same difference increases to 20% in the case of GGA + U (cf figure 6(d)). Similarly, and even more markedly, the occupation of the out-of-plane e_g orbital is 20% higher for Mn_2 and further increases within GGA+U (cf figures 6(e) and (f)). This is expected to have consequences on the ferromagnetism (although it is hard to give a quantitative estimate on the reduction of T_C induced by the different occupations): in particular, upon compressive strain, the resulting lower transfer integral for the more-occupied $3z^2 - r^2$ orbital should suppress the in-plane carrier density and, as a consequence, double-exchange hopping and T_C, whereas, as already pointed out, a smaller in-plane MnO bond length should lead to an opposite tendency.

Finally, we briefly comment on the effects of the Jahn–Teller Q_3-like distortions [29] (i.e. octahedral elongation) for $LSMO_{LAO}$, $LSMO_{NGO}$ and $LSMO_{LAO}$, in particular on the magnetic moments. In figure 7 we plot the magnetic moments (on the two Mn atoms and total moment per unit cell in panels (b), (c) and (a), respectively) as a function of the c lattice constant for LSMO on the LAO, NGO and STO substrates; we also show the experimental

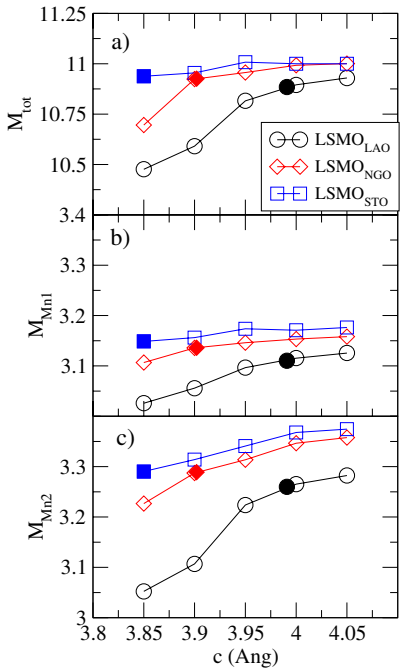

Figure 7. (a) Total, (b) Mn_1 and (c) Mn_2 magnetic moments (in Bohr magnetons) as a function of the out-of-plane lattice constant (in Å) for $LSMO_{LAO}$ (black circles), $LSMO_{NGO}$ (red diamond) and $LSMO_{STO}$ (blue squares). Filled symbols show the values obtained for the experimental equilibrium structure.

equilibrium structures using filled symbols. As previously noted, the situation in $LSMO_{LSAT}$ is very similar to $LSMO_{NGO}$ and is therefore not shown. It is worthwhile remarking that, whereas moments in $LSMO_{STO}$ are basically unaltered by the out-of-plane lattice constants, $LSMO_{NGO}$ shows slightly larger strain-induced effects and in $LSMO_{LAO}$ the dependence on c is rather significant. This is consistent with the related electronic structure: whereas LSMO on STO is always very close to half-metallicity for all the considered c values, this condition is by far 'less satisfied' in LSMO grown on LAO. This has a relatively big effect on the magnetic moments: especially for lower c values, there is an appreciable density of states coming from the minority conduction bands that cross E_F, therefore becoming occupied and lowering the total as well as Mn-projected magnetic moment.

5. Conclusions

First-principles calculations have been performed on LSMO grown on different experimentally common substrates, in order to highlight the effects of uniaxial or biaxial strain on the electronic and magnetic structure. Our results show that: (i) GGA does not exactly reproduce the experimental structural parameters, such as the out-of-plane lattice constant, and the inclusion of correlation effects according the GGA + U formalism does not significantly alter the situation. However, the discrepancy (at most of the order of 1.3%) falls within the generally acknowledged error range of density functional calculations and might also be due to defects in the experimental samples; (ii) in none of the considered substrates do we obtain full half-metallicity within bare GGA. However, even the inclusion of a small Hubbard parameter $U \sim$ 2–3 eV—consistent with recent experiments—turns the system into a 100% spin-

polarized density of states at the Fermi level, in agreement with experiments and for all the considered substrates. Moreover, within bare GGA, $LSMO_{STO}$ is closer to half-metallicity than $LSMO_{LAO}$: the minority t_{2g} states, whose tails cross the Fermi level preventing full half-metallicity, have increasingly higher excited-state energies as the tensile strain grows. In summary, strain effects (at least in the experimentally accessible range) on the relevant electronic and magnetic properties, such as the half-metallic gap and the magnetic moments, do not significantly change the overall picture. However, subtle effects such as the occupation of the in-plane versus out-of-plane e_g orbital, that are quantitatively estimated in the case of $LSMO_{LAO}$ and $LSMO_{STO}$, can change the magnetic coupling dramatically. These results call for further investigations on the strain-induced effects on the ferromagnetic exchange constants.

Acknowledgments

CM gratefully acknowledges kind hospitality from CNR-INFM CASTI regional laboratory, where part of this work was performed. We thank Professor Dr S Bluegel and Dr G Bihlmayer (Forschungszentrum Juelich, Germany) for interesting discussions. The work is partly supported by the National Natural Science Foundation of China under Grant No. 10304002.

References

[1] Jonker G H and Van Santen J H 1950 *Physica* **16** 337
[2] Salamon M B and Jaime M 2001 *Rev. Mod. Phys.* **73** 583
[3] Coey J M D, Viret M and Von Molnar S 1999 *Adv. Phys.* **48** 167
[4] Bowen M, Bibes M, Barthelemy A, Contour J P, Anane A, Lemaitre Y and Fert A 2002 *Appl. Phys. Lett.* **82** 233
Bowen M, Barthelemy A, Bibes M, Jacquet E, Contour J P, Fert A, Ciccacci F, Duo L and Bertacco R 2005 *Phys. Rev. Lett.* **95** 137203
[5] Millis A J, Darling T and Migliori A 1997 *J. Appl. Phys.* **83** 1589
[6] Tsui F, Smoak M C, Nath T K and Eom C B 2000 *Appl. Phys. Lett.* **76** 2421
[7] Kwon C *et al* 1997 *J. Magn. Magn. Mater.* **172** 229
[8] Ranno L, Llober A, Tiron R and Favre-Nicolin E 2002 *Appl. Surf. Sci.* **188** 170
[9] Lee Y P, Park S Y, Prokhorov V G, Komashko V A and Svetchnikov V L 2004 *Appl. Phys. Lett.* **84** 777
[10] Maurice J L, Pailloux F, Barthelemy A, Durand O, Imhoff D, Lyonnet R, Rocher A and Contour J P 2003 *Phil. Mag.* **83** 3201
[11] Bertacco R, Riva M, Cantoni M, Signorini L and Ciccacci F 2005 *Appl. Phys. Lett.* **86** 252502
[12] Zhang J, Tanaka H, Kanki T, Choi J H and Kawai T 2001 *Phys. Rev.* B **64** 184404
[13] Singh D J and Pickett W E 1998 *Phys. Rev.* B **57** 88
Singh D J and Pickett W E 1998 *J. Appl. Phys.* **83** 7354
[14] Livesay E A, West R N, Dugdale S R, Santi G and Jarlborg T 1999 *J. Phys.: Condens. Matter* **11** L271
[15] Banach G and Temmerman W M 2004 *Phys. Rev.* B **69** 054427
[16] Zenia H, Gehring G A, Banach G and Temmerman W M 2005 *Phys. Rev.* B **71** 024416
[17] Geng T and Zhang N 2006 *Phys. Lett.* A **351** 314
[18] Perdew J P, Burke K and Ernzerhof M 1996 *Phys. Rev. Lett.* **77** 3865
[19] Wimmer E, Krakauer H, Weinert M and Freeman A J 1981 *Phys. Rev.* B **24** 864
[20] http://www.flapw.de
[21] Anisimov V I, Aryasetiawan F and Lichtenstein A I 1997 *J. Phys.: Condens. Matter* **9** 767
[22] Shick A *et al* 1999 *Phys. Rev.* B **60** 10763
[23] Singh D J 1991 *Phys. Rev.* B **43** 6388
[24] Monkhorst H J and Pack J D 1976 *Phys. Rev.* B **13** 5188
[25] Chikamatsu A, Wadati H, Kumigashira H, Oshima M, Fujimori A, Hamada N, Ohnishi T, Lippmaa M, Ono K, Kawasaki M and Koinuma H 2005 *Preprint* cond-mat/0503373
[26] Souza-Neto N M, Ramos A Y, Tolentino H C N, Favre-Nicolin E and Ranno L 2004 *Phys. Rev.* B **70** 174451
[27] Ederer C and Spaldin N A 2005 *Phys. Rev.* B **71** 224103
[28] Ma C, Yang Z Q and Picozzi S, unpublished
[29] Ahn K H and Millis A J 2001 *Phys. Rev.* B **64** 115103